# Electric field induced self-assembled nanostructures in spray deposited nanocrystalline CdX and HgX (X= Se and Te) thin films

**V. Dutta* and A. Ranga Rao**

Photovoltaic Laboratory, Centre for Energy Studies, Indian Institute of Technology Delhi, Hauz Khas, New Delhi-110016, India

*Corresponding author E-mail ID: vdutta@ces.iitd.ernet.in

## ABSTRACT

Self assembling in Nanocrystalline CdX and HgX (X=Se and Te) thin films prepared by spray deposition have been reported due to the presence of electric filed during the deposition. The films are prepared using Solvothermally synthesized nanoparticles dispersed in 1-Butanol and sprayed on the glass substrates at 200°C without any voltage as well as by applying a voltage to the nozzle. The electron microscopy studies reveal the formation of randomly distributed nanoparticles for the films deposited without voltage and nanorods for the films deposited with voltage. The formation of nanorods is found to be a function of the ionicity of the materials. X-ray diffraction studies of CdSe films reveal formation of hexagonal crystal structure for the films deposited both without voltage and with voltage. CdTe film deposited without voltage show the cubic crystal structure and the films deposited with voltage show hexagonal crystal structure. X-ray diffractograms of HgX films deposited without and with voltage show cubic crystal structure of HgX. HRTEM studies clearly show lattice planes of the corresponding crystal structures. In view of the self assembly observed under voltage and the difference between CdX and HgX, dipole-dipole interaction can be the driving force for the nanoparticles converting into the nanorods.

## 1. INTRODUCTION

Semiconductor nanorods and nanowires exhibit novel electronic and optical properties due to their unique structural one-dimensionality and possible quantum confinement effects. These one-dimensional semiconductor nanostructures are considered to be the critical components in a wide range of potential nanoscale devices. Among them II-VI semiconductor nanostructures have been found applications in various devices like inorganic solar cells, hybrid solar cells, biological tagging [1-4]. To fully exploit these one-dimensional nanostructures, current research is focused on controlled synthesis of one-dimensional nanoscale building blocks, and integration of nanostructure elements into complex functional architectures. Self-assembly has been extensively explored for generating complex nanostructures on various scales [5-13]. In addition to self-assembly, external manipulation with a field or a mechanical probe has also been explored to induce or direct the organization of nanoparticles into arrayed structures [14-19].

Self-assembling system can be defined as the one in which the individual components interact in pre-defined ways that result in the spontaneous self-organization of those components into higher-order structures. Self-assembly happens extensively in Nature. From molecules to much more complex biological systems, self-assembly contributes to making patterns, ordered objects, and functional systems. Self-assembly as a nanofabrication method offers a number of advantages. 1) Self-assembly is inherently a parallel process. This feature is particularly important at the nano-scale. As the length scale of devices shrink to smaller sizes, it becomes exceedingly difficult to manipulate individual components. 2) Self-assembly at the molecular level can generate structures with sub-nanometer precision. 3) Self-assembly at the molecular level offers the ability to generate three-dimensional (3-D) architectures. 4) External forces and geometrical constraints can alter the outcome of a self-assembly process. Two main steps are involved in designing a system that takes advantage of self-assembly for fabrication. First, the interaction between the elements that constitute the final system should be modified for the proper response. The interaction between the elements (molecules, particles) in the system can be controlled using chemistry. Typically, the chemistry involves hydrogen bonding, van der Waals forces, electrostatic forces, or hydrophobic interactions. The internal interaction of the elements does not uniquely define the final state of a self-organizing system. External forces and geometrical constrains can change the outcome of a self-assembly process, and provide flexibility to process into different designs. The second step in the design of a self-assembling system is to determine external parameters in order to guide the process and achieve the desired result. For example, electrostatic, magnetic, or hydrodynamic forces can be employed to guide a self-assembly process towards a particular application. Spray deposition can be a convenient process in creating self assembly of nanoparticles, since the atomization can be done by charging the droplets which in turn allows the charged nanoparticles to suitably create nanorods etc [20]. In this paper we report on the electric field induced self-assembled nanostructures in spray deposited CdX and HgX thin films. The role of ionicity and the resultant dipole-dipole interaction in the creation of self-assembled nanostructures will be discussed.

## 2. EXPERIMENTAL DETAILS

CdX and HgX nanoparticles have been synthesized using solvothermal method [21]. Thus prepared nanoparticles have been dispersed in 1-Butanol for spray solution, and the solution is sprayed on the glass substrates kept in air at 200°C. The distance between the substrates and the nozzle is maintained at 20 cm, the solution flow rate is maintained at 1.5 ml/min. Nitrogen is used as a carrier gas. Deposition has been

done without and with applying an external voltage (300V-3kV) to the nozzle and the metal electrode placed 2 mm below the nozzle [22]. Structural and Morphological studies of the films have been done using RIGAKU Giegerflex-D X-ray diffractometer, Philips CM 12 Transmission Electron Microscopy. For TEM studies the samples are prepared by depositing the films on NaCl crystals ~ 100A° thick, and then lifted on to the carbon coated copper (300 mesh) grid, the samples are dried under vacuum for 3 hrs. HRTEM studies have been done using JEOL 2010 200KeV Transmission electron microscopy.

## 3. RESULTS AND DISCUSSION

### 3.1 Structural Studies

Fig.1 shows the X-ray diffractograms of the CdX and HgX films deposited without and with voltage. For simplicity the data for films deposited without voltage and with 700V have been given. CdSe films deposited without and with voltage show the hexagonal crystal structure with (002) as dominant peak. In case of CdTe, films deposited without voltage show the cubic crystal structure with (111) as dominant peak, whereas, the films deposited with voltage show the hexagonal crystal structure. In both the films $CdTeO_3$ peaks are also present; the amount of $CdTeO_3$ is increasing in case of the films deposited with voltage. There are earlier reports on oxygen induced phase transition from cubic to hexagonal phase CdTe [23, 24]. However, in our case the presence of $CdTeO_3$ in both the films suggests that the voltage is helping towards the stabilization of meta-stable hexagonal phase. Interestingly, the films deposited with intermediate voltages also show the hexagonal phase CdTe. In case of HgSe and HgTe films deposited without and with voltage show the cubic crystal structure with (111) as dominant peak for both the films. The lattice parameters calculated for all the materials are close to the standard values.

### 3.2 Morphological Studies

Figures 2 and 3 show the TEM images of the CdX films deposited without voltage and with voltage. The TEM images of the CdSe and CdTe films deposited without voltage show spherical nanoparticles of average particle size of ~8 and ~10nm for CdSe and CdTe, respectively. The lattice parameters calculated from the electron diffraction pattern recorded on these images is found to be - CdSe: a = 0.429 nm, c = 0.703 nm; CdTe: a=0.645 nm - these match with values obtained from the X-ray diffraction studies. This is also confirmed by HRTEM images of the films, where we can clearly see the lattice resolution of the individual nanoparticles, which are assigned to (002) phase in case of CdSe and (111) phase for CdTe.

On the other hand, the films deposited with voltage show nanorod morphology. In case of CdSe, less voltage (300V) is needed to obtain the nanorod morphology (diameters 20-50 nm). There is no exact trend in the aspect ratio with the increase in the applied voltage, as the films show randomly distributed nanorods, each nanorod with different aspect ratio at each voltage under which the films are deposited. There is a little increase in the aspect ratio with the increase in voltage (the diameter of the nanorods decreases and the length of the rods increase). The HRTEM image of a single CdSe nanorod (fig.2(c)) shows the lattice resolution of the nanorods and the growth axis is found to be in the [002] direction of the lattice, this supports the X-ray diffraction data. Fig.3 shows how the nanorods evolution of CdTe from spherical nanoparticles takes place. Nanorod formation started at 300V (diameters 50-100nm) with smaller aspect ratio and the completion of the full nanorods formation is taking place at higher voltages (>=700V). The films deposited with 700V show the presence of hexagonal CdTe nanorods of width ~ 20nm and length ~ 5$\mu$m. The lattice resolution from HRTEM image(fig.3(d)) of the single nanoparticle of CdTe deposited without voltage shows the cubic crystal structure with [111] direction of growth axis, whereas, that of isolated nanorod seen in the films deposited under voltage corresponds to that of hexagonal CdTe having the [002] direction of the growth axis as seen in the X-ray data.

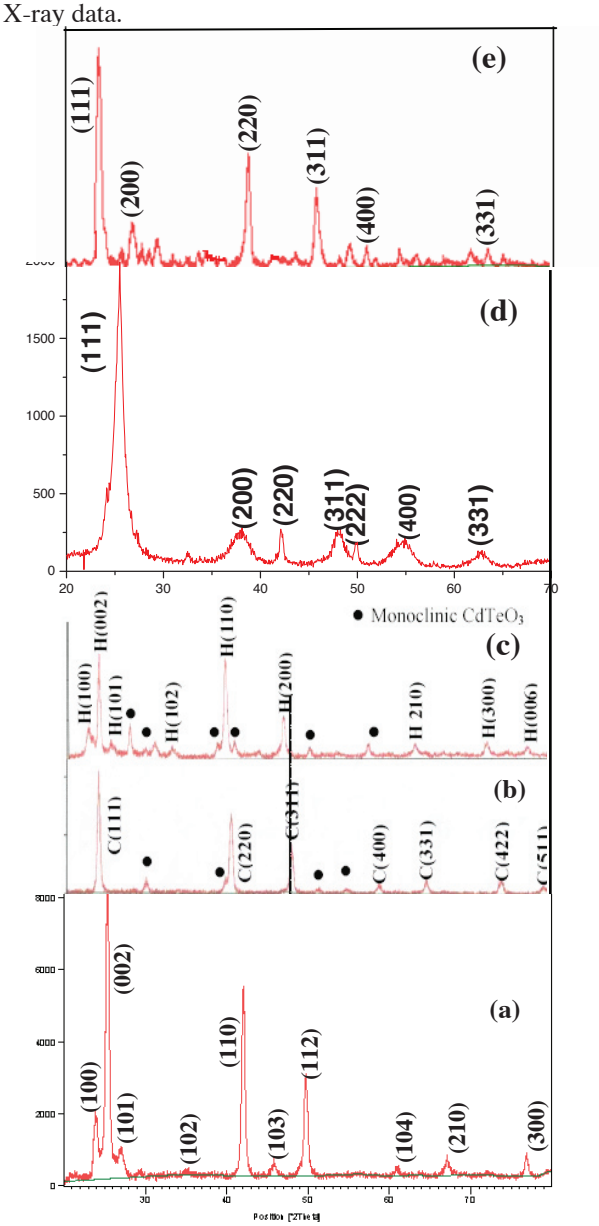


Fig.1 X-ray diffractograms of the CdSe films deposited (a) without voltage (b) CdTe without voltage (c) CdTe 700V (d) and (e) HgSe and HgTe without voltage

It should be pointed out that in case of CdTe a higher voltage has to be applied in order to obtain the nanorods compared to that for CdSe.

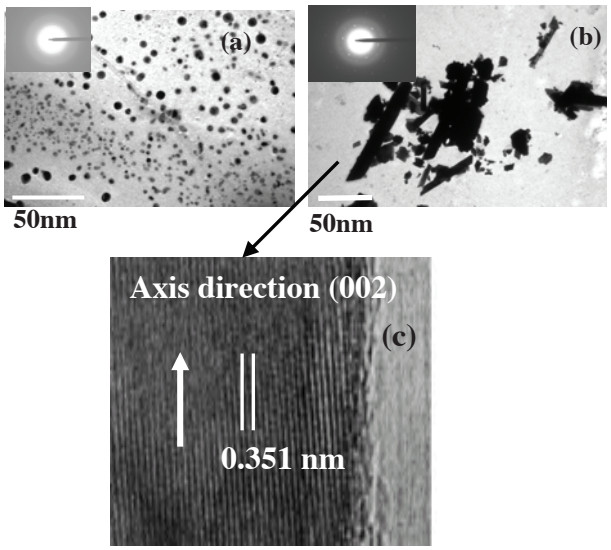


Fig. 2 TEM images of CdSe films deposited with (a) without voltage (b) with 300V(c) HRTEM image of individual nanorod

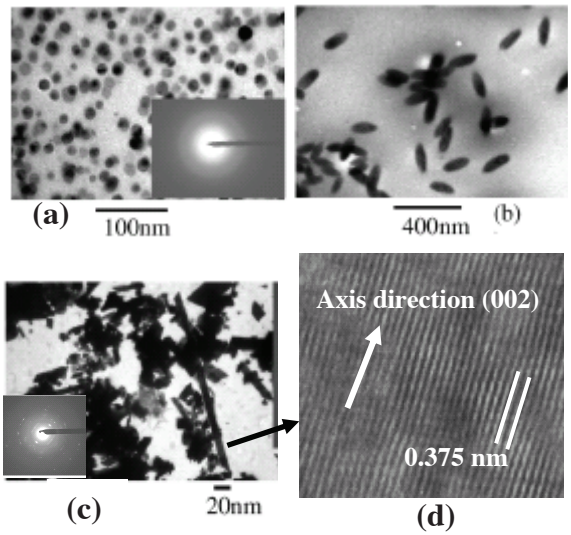


Fig.3 TEM images of CdTe films deposited with (a) without voltage (b) 400V(c) 700V and (d) HRTEM image of individual nanorod

The reason for this difference can be due to the difference in the ionicity of respective materials. Since the ionicity of CdSe is more (78%) than that of the CdTe (72%), it may be easy to induce dipole moment in CdSe compared to CdTe. Moreover with materials in nanoscale the ionicity increases which may further help the process [25]. Ionicity is more in case of materials with hexagonal phase compared to cubic phase materials, which can also help in stabilization of hexagonal CdTe phase [3, 26]**.** Hence, there is a possibility of creation of permanent dipole and dipole-dipole interaction in the materials deposited under the electric field. In turn this helps in the creation of nanorods and other nanostructures.

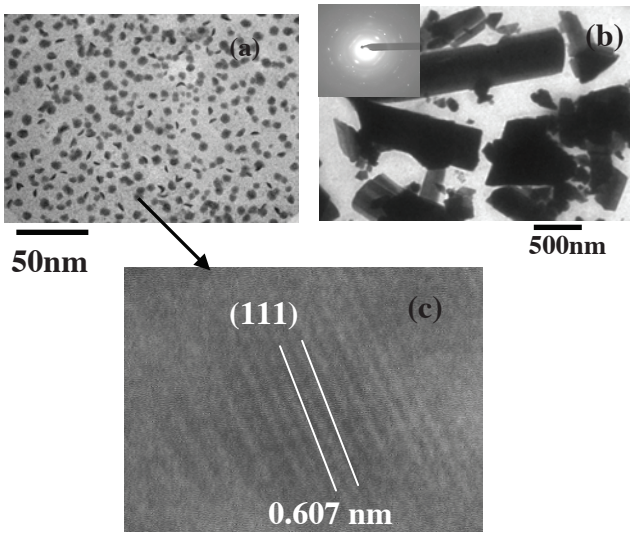


Fig. 4 TEM images of HgSe films deposited with (a) without voltage (b) with 700V(c) HRTEM image of individual nanoparticle

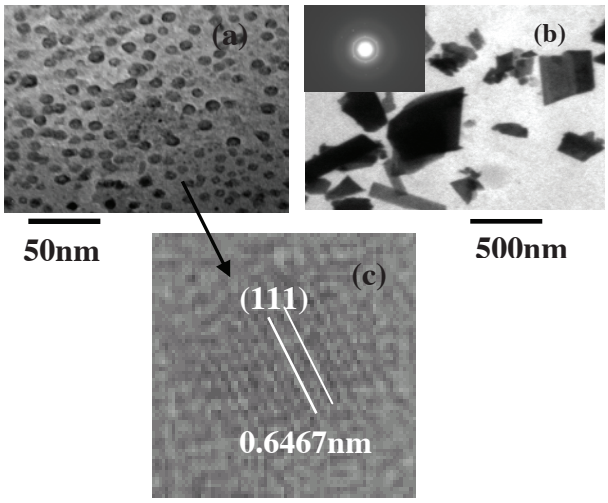


Fig. 5 TEM images of HgTe films deposited with (a) without voltage (b) with 700V(c) HRTEM image of individual nanoparticle

One way of confirming this observation will be to do the deposition for a material with lesser ionicity and see the role of voltage in promoting self-assembly in these films. We have chosen HgX (X = Se, Te) which shows less ionicity (<65%) compared to that of CdX. In addition, nanoparticles of HgX can also be conveniently prepared by solvothermal method. TEM images of the HgX films deposited without voltage show the formation of randomly distributed nanoparticles with average particle size of ~8 and ~12 nm for HgSe and HgTe respectively. HgSe and HgTe films deposited under voltage

show the formation of submicron rods (300-600nm), however the voltage needed to create this morphology is higher (1kV) compared to that for CdX case. As mentioned before, the ionicity of these materials is less which reduces the possibility of dipole-dipole interaction needed for the creation of nanorods. The lattice parameters for HgSe and HgTe calculated from the SAD pattern is found to be 0.6063 nm and 0.6463 nm respectively, matching the standard value. The HRTEM measurements on these films clearly show the lattice resolution, with growth axis in the direction of [111] for both HgTe and HgSe (fig.4(c) and 5(c)). This confirms that the films are of highly crystalline with cubic crystal structure. HRTEM images of HgSe and HgTe films deposited with voltage also show the cubic crystal structure.

Our observations show that the nanoparticles in the spray droplets are influenced by the presence of the electric field giving rise to dipoles. After the solvent gets evaporated on the heated substrate, the dipole-dipole interaction leads to nanorod formation. The other possible mechanism can be due to the van der Waals forces. But it should be pointed out that the van der Waals force exists in the II-VI nanoparticle system is quite weak and the energy of the nanoparticles is estimated to be less than 0.5 RT, which is not enough to stabilize the nanoparticle superstructures under ambient conditions [26]. Further, the voltage necessary to promote nanostructure formation through dipole-dipole interaction depends on the material used. This can be explained by taking into account the fact that the magnitude of dipole moment of CdX is high as compared to HgX [27].

## CONCLUSIONS

CdX and HgX thin films have been prepared without and with applying a voltage by spray deposition method using solvothermally synthesized nanoparticles. The voltage is found to help in the creation of self-assembled nanorod structures through dipole-dipole interactions. Ionicity of the materials is found to play a major role in promoting this interaction. The presence of these dipoles can be conveniently exploited in orienting the nanorods formation in the desired direction. Thus prepared nanorods can be used for different devices for example in inorganic solar cells and in the hybrid solar cells for better light harvesting and carrier transport.

## ACKNOWLEDGMENT

One of the authors (A.R.) thanks MNRE, New Delhi, India, for awarding a research fellowship. Authors are grateful to the Electron Microscopy Division, Department of Anatomy, All India Institute of Medical Sciences (AIIMS), New Delhi, for the SEM and TEM measurements. Authors thank Prof. Satyam, IOP, Bhubaneswar, India for HRTEM measurements.

## REFERENCES

1. I. Gur, N.A. Fromer, M.L. Geier, A.P. Alivisatos, Science, 310, 462, 2005.
2. W.U. Huynh, J.J. Dittmer and A.P. Alivisatos, Science, 295, 2427, 2002.
3. X. Michalet, F.F. Pinaud, L.A. Bentolila, J.M. Tsay, S. Doose, J.J.Li.G. Sundaresan, A.M. Wu, S.S. Gambhir and S. Weiss, Science 307, 538, 2005.
4. L. Manna, D.J. Milliron, A. Meisel, E.C. Scher, and A.P. Alivisatos, Nat. Mater. 2, 382(2003).
5. W. Noll J. Inorg. Chem. 261, 1, 1950.
6. J. M. Tarascon, J.J. Disalvo, C.H. Chen, P.J. Carrol, M. Walsh, and L. Rupp., J. Solid State Chem. 58, 290, 1985.
7. B. Messer, J.H. Song, M. Huang, Y. Wu, F. Kim, and P. Yang, Adv. Mater., 12, 1526, 2000.
8. J. Song, B. Messer, Y. Wu, H. Kind and P. Yang, J. Am. Chem.Soc., 123, 9714, 2001.
9. Z. Zhang, D. Gekhtman, M.S. Dresselhaus, J.Y. Ying, Chem. Mater. 11, 1659, 1999.
10. S.J. Limmer, S. Seraji, Y. Wu, T.P. Chou, C. Nguyen and G. Cao, Adv. Funct. Mater. 12, 59, 2002.
11. V. M. Cepak and C. R. Martin, Chem. Mater. 11, 1363, 1999.
12. P. Hoyer, N. Baba and H. Masuda, Appl. Phys. Lett. 1995, 66, 2700.
13. P. Swaminathan, V.N. Antonov, J.A.N.T. Soares, J.S. Palmer and J.H. Weaver, Phys Rev B, 2006, 73, 125430.
14. M. Trau, S. Sankaran, D.A. Saville and I.A. Aksay, Nature, 374, 437, 1995.
15. M. Trau, N. Yao, E. Kim, Y. Xia, G.M. Whitesides and I. A. Aksay, Nature, 390, 674, 1997.
16. S. H. Tolbert, A. Firouzi, G.D. Stucky and B.F. Chmelka, Science, 278, 264, 1997.
17. N.A. Melosh, P. Davidson, P. Feng, D.J. Pine and B.F. Chmelka, J. Am. Chem. Soc. 123, 1240, 2001.
18. Y. Kawashima, M. Nakagawa, T. Seki and K. Ichimura, Chem. Mater. 14, 2842, 2002.
19. Y. Lu, R. Ganguli, C.A. Drewien, M.T. Anderson, C.J. Brinker, W.L. Gong, Y.X. Guo, H. Soyez, B. Dunn, M.H. Huang and J.I. Zink, Nature, 389, 364, 1997.
20. A. Ranga Rao and V. Dutta, phys. stat. sol(a) 201, R72 2004.
21. A. Ranga Rao and V. Dutta, Phys.stat.sol (a), 203, 854, 2006.
22. K. Vamsi Krishna and V. Dutta, Thin solid films, 444, 17 2003.
23. H. A. Chavez, F. J. E. Beltran, R. R. Bon, O. Z. Angel and G. Hernandez, J. Solid State Commun. 101, 39, 1997.
24. P. Babu Dayal, B. R. Mehta, Y. Aparna and M. Shivaprasad, Appl. Phys. Lett. 81, 4254, 2002.
25. Z. Tang, N. A. Kotov and M. Giersig, Science, 297, 237, 2002.
26. B. A. Korgel and D. Fitzmaurice, Adv. Mater. 10, 661, 1998.
27. M. Shim and P.G. Sionnest, J. Chem. Phys. 111, 6955, (1999).